Harmful Algae
May 2016, Volume 55 Pages 56-65
https://doi.org/10.1016/j.hal.2016.02.006
https://archimer.ifremer.fr/doc/00316/42682/

Morphology, molecular phylogeny and azaspiracid profile of *Azadinium poporum* (Dinophyceae) from the Gulf of Mexico

Luo Zhaohe [1, 2], Krock Bernd [3, *], Mertens Kenneth [4, 8], Price Andrea Michelle [5], Turner Robert Eugene [6], Rabalais Nancy N. [7], Gu Haifeng [2, *]

[1] Jinan Univ, Coll Life Sci & Technol, Guangzhou 510632, Guangdong, Peoples R China.
[2] SOA, Inst Oceanog 3, Xiamen 361005, Peoples R China.
[3] Alfred Wegener Inst Polar & Marine Res, Handelshafen 12, D-27570 Bremerhaven, Germany.
[4] Univ Ghent, Res Unit Palaeontol, Krijgslaan 281 S8, B-9000 Ghent, Belgium.
[5] McGill Univ, Dept Geog, Burnside Hall,805 Sherbrooke St West, Montreal, PQ H3A 0B9, Canada.
[6] Louisiana State Univ, Dept Oceanog & Coastal Sci, Baton Rouge, LA 70803 USA.
[7] Louisiana Univ Marine Consortium, Chauvin, LA 70344 USA.
[8] LER BO, Stn Biol Marine, Pl Croix,BP40537, F-29185 Concarneau, France.

* Corresponding author : Bernd Krock, email address : bernd.krock@awi.de ; Haifeng Gu, email address : guhaifeng@tio.org.cn

Abstract :

Azadinium poporum produces a variety of azaspiracids and consists of several ribotypes, but information on its biogeography is limited. A strain of A. poporum (GM29) was incubated from a Gulf of Mexico sediment sample. Strain GM29 was characterized by a plate pattern of po, cp, x, 4′, 3a, 6″, 6C, 5S, 6‴, 2⁗, a distinct ventral pore at the junction of po and the first two apical plates, and a lack of an antapical spine, thus fitting the original description of A. poporum. The genus Azadinium has not been reported in waters of the United States of America before this study. Molecular phylogeny, based on large subunit ribosomal DNA (LSU rDNA) and internal transcribed spacer (ITS) sequences, reveals that strain GM29 is nested within the well-resolved A. poporum complex, but forms a sister clade either to ribotype B (ITS) or ribotype C (LSU). It is, therefore, designated as a new ribotype, termed as ribotype D. LSU and ITS sequences similarity among different ribotypes of A. poporum ranges from 95.4% to 98.2%, and from 97.1% to 99.2% respectively, suggesting that the LSU fragment is a better candidate for molecular discrimination. Azaspiracid profiles were analyzed using LC–MS/MS and demonstrate that strain GM29 produces predominantly AZA-2 with an amount of 45 fg/cell. The results suggest that A. poporum has a wide distribution and highlights the risk potential of azaspiracid intoxication in the United States.

Highlights

► The genus *Azadinium* is reported for the first time in waters of USA. ► *Azadinium poporum* from the Gulf of Mexico represents a new ribotype. ► *Azadinium poporum* from the Gulf of Mexico produces predominantly AZA-2.

Keywords : AZA-2, AZA-2 phosphate, Biogeography, LC-MS/MS, LSU rDNA, Ribotype D

1. Introduction

The known diversity of the dinophyte genus *Azadinium* Elbrächter & Tillmann has increased rapidly. Up to ten species have been described in the past five years (Tillmann et al., 2009; Tillmann et al., 2010; Tillmann et al., 2011; Luo et al., 2013; Percopo et al., 2013; Tillmann et al., 2014). Additionally, *Amphidoma caudata* Halldal has been transferred to *Azadinium* based on both morphology and molecular phylogeny (Nézan et al., 2012). The genus *Azadinium* was characterized by a plate pattern of po, cp, x, 3-4′, 2-3a, 6″, 6C, 5S, 6‴, 2⁗ (Tillmann et al., 2009, Luo et al., 2013), in which the presence of anterior intercalary plates and a canal plate resembles the Peridiniales and the presence of six precingular and postcingular plates resembles the Gonyaulacales. In the molecular phylogeny, the genus *Azadinium* is monophyletic and forms an independent lineage together with *Amphidoma* Stein, which is classified within the family Amphidomataceae, but its higher level designation remains to be determined (Tillmann et al., 2012*a*; Tillmann et al., 2014).

Most *Azadinium* species were described from samples collected in European waters, but that does not mean that there is a restricted distribution of these small dinoflagellates. For example, *A. spinosum* was also reported in the Mexican Pacific (Hernández-Becerril et al., 2012), and *A. poporum* was found in Korea (Potvin et al., 2011), China (Gu et al., 2013), New Zealand (Smith et al., 2015) and Argentina (Tillmann et al., 2016). *Azadinium* diversity might be underestimated because their cells are rather small and molecular detection is not routinely carried out (Toebe et al., 2013).

68 The type species of *Azadinium* (*A. spinosum*) was related to azaspiracids (AZA-1
69 and AZA-2) and thus was the organism responsible for cases of human intoxication
70 via mussel consumption (Tillmann et al., 2009). Later, two other species (*A.*
71 *dexteroporum*, *A. poporum*) were found to contain AZAs too (Percopo et al., 2013; Gu
72 et al., 2013; Krock et al., 2014). It is worth noting that *A. poporum* comprises several
73 genetically different ribotypes that are morphologically identical. The strains from
74 Europe and New Zealand share identical sequences and belong to ribotype A, whereas
75 those from Korea, China and Argentina belong to ribotype B or C (Gu et al., 2013;
76 Smith et al., 2015; Tillmann et al., 2016). Additional ribotypes can be expected to be
77 discovered because only a limited number of *A. poporum* strains have been
78 sequenced.
79 The presence of azaspiracids (AZA) has been reported in mussels of northern
80 Africa (Taleb et al., 2006), mussels from northern Europe (Satake et al., 1998),
81 scallops and mussels from Chile (Lopez-Rivera et al., 2010), a marine sponge from
82 Japan (Ueoka et al., 2009), shellfish from China (Yao et al., 2010), shellfish from New
83 Zealand (Smith et al., 2015) and plankton samples from the Pacific coast of the USA
84 (Trainer et al., 2013). However, AZA producing species have not been reported in
85 some of these areas, e.g., from the USA. Incubated sediment samples from the
86 northern Gulf of Mexico, generated one strain of *A. poporum*. Its morphology was
87 examined in detail, and its partial large subunit ribosomal DNA (LSU rDNA) and
88 internal transcribed spacer regions (ITS) sequences were determined. This strain was
89 also grown in larger quantities and analyzed for the presence of AZAs.

2. Material and methods

2.1. Sample collection and treatment

A box core was collected from the northern Gulf of Mexico (29.3250°N, 93.4167°W, water depth: 17.3 m) on August 1, 2014. The top 2 cm were sliced off and stored in the dark at 4 °C until further treatment. Approximately 5 g of wet sediment was mixed with 20 mL of filtered sea water and sonicated for 2 min (100 W) to dislodge detrital particles. The watery slurry was incubated directly in a series of small containers in f/2-Si medium (Guillard and Ryther, 1962) at 20 ºC, 90 $\mu E \cdot m^{-2} \cdot s^{-1}$ under a 12:12 h light: dark cycle (hereafter called "standard culture conditions"). *Azadinium* cells are characterized by swimming at low speed, interrupted by short, high-speed 'jumps' in various directions (Tillmann et al., 2009). Cells exhibiting such a characteristic swimming behavior were isolated by means of drawn-out Pasteur pipettes and established in clonal cultures. Only one strain (GM29) was established from one container, and it was maintained under standard culture conditions.

2.2. Light microscopy (LM)

Live cells were examined under a Zeiss Axio Imager microscope (Carl Zeiss, Göttingen, Germany) equipped with both differential interference illumination and epifluorescence. Light micrographs were obtained using a Zeiss AxiocamHRc digital

camera. Approximately 1 mL of live, healthy culture in mid exponential growth phase was transferred to a 1.5 mL microcentrifuge tube, and stained with 1: 100 000 Sybr Green (Sigma-Aldrich, St. Louis, USA) for 10 min. The cells were viewed and photographed through a Zeiss Filterset (excitation BP 450-490; beamsplitter FT 510; emission LP 515). Cells in mid-exponential growth phase were fixed with 5% Lugol's solution and cell sizes were measured at 400× magnification. Thirty cells were measured for the strain GM29.

2.3. Scanning electron microscopy (SEM)

Mid-exponential batch cultures were collected by centrifugation at 5,000 rpm to use for scanning electron microscopy (SEM). The supernatant was removed and the cell pellet that was re-suspended in 60% ethanol for 1 h at 8 ºC to strip off the outer cell membrane. The cells were pelleted by centrifugation and re-suspended in filtered sea water for 30 min at 8 ºC. Cell pellets were re-suspended and fixed with 2.5% glutaraldehyde prepared with f/2-Si medium for 3 h at 8 ºC. Cell pellets were washed twice with f/2-Si medium and fixed overnight at 8 ºC with 2% OsO_4 made up with filtered sea water. The supernatant was removed and the cell pellet was allowed to adhere to a coverslip coated with poly-L-lysine (molecular weight 70,000–150,000). The attached cells were washed for 10 min in a 1:1 solution of distilled water and filtered sea water, followed by a second wash in distilled water lasting 10 min. The samples were then dehydrated in a series of ethanol (10, 30, 50, 70, 90and 3× in 100%, 10 min at each step), critical point dried (K850 Critical Point Dryer, Quorum/Emitech,

West Sussex, UK), sputter-coated with gold, and examined with a Zeiss Sigma FE (Carl Zeiss Inc., Oberkochen, Germany) scanning electron microscope.

2.4. PCR amplifications and sequencing

The total algal DNA was extracted from 10 mL of exponentially growing *Azadinium* cultures using a plant DNA extraction kit (Sangon, Shanghai, China) according to the manufacturer's protocol. PCR amplifications were carried out using 1× PCR buffer, 50 μM dNTP mixture, 0.2 μM of each primer, 10 ng of template genomic DNA, and 1 U of ExTaq DNA Polymerase (Takara, Tokyo, Japan) in 50 μL total volume reactions. The total ITS1–5.8S–ITS2 was amplified using ITSA and ITSB primers (Adachi et al., 1996). Approximately 1400 bp of the LSU rDNA (D1–D6) was amplified using the primers of D1R (Scholin et al., 1994) and 28-1483R (Daugbjerg et al., 2000). The PCR protocol was as follows: initial denaturation for 3.5 min at 94ºC, followed by 35 cycles of 50 s denaturation at 94ºC, 50 s annealing at 45ºC, and 80 s extension at 72ºC, plus a final extension of 10 min at 72ºC. PCR products were sequenced directly in both directions using the ABI Big-Dye dye-terminator technique (Applied Biosystems, Foster City, CA, USA), according to the manufacturer's recommendations. New sequences were deposited in the GenBank with accession numbers XXXXXX and XXXXXX.

2.5. Sequence alignment and phylogenetic analysis

Newly obtained LSU rDNA and ITS sequences of *A. poporum* were aligned with

the related sequences download from GenBank using the MAFFT v7.110 (Katoh et al., 2005) online program (http://mafft.cbrc.jp/alignment/server/). Alignments were manually checked with BioEdit v. 7.0.5 (Hall, 1999). The program Jmodeltest (Posada, 2008) was used to select the most appropriate model of molecular evolution with the Akaike information criterion (AIC). This test chose the TIM1+I+G and TIM2+G models for LSU and ITS, respectively. A Bayesian reconstruction of the data matrix was performed with MrBayes 3.1.2 (Ronquist and Huelsenbeck, 2003) using the best-fitting substitution model. Four Markov chain Monte Carlo (MCMC) chains ran for one million generations, with sampling every 1,000 generations. A majority rule consensus tree was created to examine the posterior probabilities of each clade. The maximum-likelihood (ML) analyses were conducted using RaxML v7.2.6 (Stamatakis, 2006) on the T-REX web server (Boc et al., 2012) using the model GTR+G. Node support was assessed with 1,000 bootstrap replicates.

2.6. Chemical analysis of azaspiracids

Cultures of *A. poporum* were grown in 200 mL Erlenmeyer flasks under standard culture conditions to conduct an AZA analysis. About 10^7 cells were collected by centrifugation at the exponential phase. Cell pellets were extracted with 300 µL acetone by reciprocal shaking at 6.5 m s^{-1} with 0.9 g lysing matrix D (Thermo Savant, Illkirch, France) in a Bio101 FastPrep instrument (Thermo Savant, Illkirch, France) for 45 s. The extracts were then centrifuged (Eppendorf 5415 R, Hamburg, Germany) at 16,100 × g at 4 °C for 15 min. Each supernatant was transferred to a 0.45-µm

pore-size spin-filter (Millipore Ultrafree, Eschborn, Germany) and centrifuged for 30 s at 800 × *g*, and the resulting filtrate was transferred into an LC autosampler vial for LC-MS/MS analysis.

2.6.1. Single reaction monitoring (SRM) measurements

Water was deionized and purified (Milli-Q, Millipore, Eschborn, Germany) to 18 MΩ cm^{-1} or better quality. Formic acid (90%, p.a.), acetic acid (p.a.) and ammonium formate (p.a.) were from Merck (Darmstadt, Germany). The solvents, methanol and acetonitrile, were high performance liquid chromatography (HPLC) grade (Merck, Darmstadt, Germany).

Mass spectral experiments were performed to survey for a wide array of AZAs. The analytical system consisted of an AB-SCIEX-4000 Q Trap, triple quadrupole mass spectrometer equipped with a TurboSpray® interface coupled to an Agilent model 1100 LC. The LC equipment included a solvent reservoir, in-line degasser (G1379A), binary pump (G1311A), refrigerated autosampler (G1329A/G1330B), and temperature-controlled column oven (G1316A).

Separation of AZAs (5 μL sample injection volume) was performed by reverse-phase chromatography on a C8 phase. The analytical column (50 × 2 mm) was packed with 3 μm Hypersil BDS 120 Å (Phenomenex, Aschaffenburg, Germany) and maintained at 20 °C. The flow rate was 0.2 mL min^{-1} and gradient elution was performed with two eluants, wherein eluant A was water and B was acetonitrile/water (95:5 v/v), and both contained 2.0 mM ammonium formate and 50 mM formic acid. The initial conditions were 8 min column equilibration with 30% B, followed by a

194 linear gradient to 100% B in 8 min, isocratic elution until 18 min with 100% B, and
195 then returning to the initial conditions until 21 min (total run time: 29 min).
196 The AZA profiles were determined in one period (0 – 18) min with curtain gas: 10
197 psi, CAD: medium, ion spray voltage: 5500 V, ambient temperature; nebulizer gas at
198 10 psi, auxiliary gas was off, the interface heater was on, the declustering potential @
199 100 V, the entrance potential @ 10 V, and the exit potential @ 30 V. The SRM
200 experiments were carried out in positive ion mode by selecting the transitions shown
201 in table 1. AZAs were calibrated against an external standard solution of AZA-2
202 (certified reference material (CRM) programme of the IMB-NRC, Halifax, Canada)
203 and expressed as AZA-2 equivalents.
204 *2.6.2. Precursor ion experiments*
205 Precursors of the fragments *m/z* 348, *m/z* 360 and *m/z* 362 were scanned in the
206 positive ion mode from *m/z* 400 to 950 under the following conditions: curtain gas at
207 10 psi, CAD at medium, ion spray voltage at 5500 V, ambient temperature, a 10 psi
208 nebulizer gas, the auxiliary gas was off, the interface heater was on, a declustering
209 potential of 100 V, a 10 V entrance potential, a 70 V collision energy, and a 12 V exit
210 potential.
211 *2.6.3. Collision Induced Dissociation (CID) spectra*
212 CID spectra of *m/z* 856 and *m/z* 936 were recorded in the Enhanced Product Ion
213 (EPI) mode in the mass range from *m/z* 150 to 960 in a positive ionization and unit
214 resolution mode. The following parameters were applied: 10 psi curtain gas, medium
215 CAD, a 5500 V ion spray voltage, ambient temperature, a 10 psi nebulizer gas, the

auxiliary gas was off, the interface heater was on, there was a 100 V declustering potential, the collision energy spread was 0 and 10 V, and the collision energy was 70 V.

3. Results

3.1. Morphology

The cells of *A. poporum* strain GM29 were 11.2–16.0 µm long (mean=13.3 ±1.2 µm, n=30) and 8.2–11.8 µm wide (mean=9.8 ±0.9 µm, n=30) with a median length: width ratio of around 1.4. The large nucleus was spherical to slightly elongated and located in the lower part of the cell (Fig. 1). Up to three pyrenoids were visible in the light microscope, and were located either in the epitheca or hypotheca (Fig. 1A). A single chloroplast was situated in the periphery of the cell (Fig. 1B).

The cells had a conical epitheca and a hemispherical hypotheca, interrupted by a deep and wide cingulum, descending less than half the cingulum width (Fig. 2A). Trichocysts were observed on the cell surface, including the cingular and sulcal plates. The cells showed a plate pattern of po, cp, x, 4′, 3a, 6″, 6C, 5S, 6‴, 2‴″. The cingulum was composed out of six plates of similar size (Fig. 2A, B). The rounded apical pore was located in the centre of a pore plate (po) and covered by a cover plate (cp) (Fig. 2C). There was a distinct ventral pore (vp) located at the junction of the apical pore and the first two apical plates (1′, 2′) (Fig. 2C). The first apical plate was not symmetrical (Fig. 2C). There were three anterior intercalary plates (1a, 2a and 3a) on the dorsal part of the epitheca. Plates 1a and 3a were pentagonal or hexagonal, much

larger than the four-sided 2a (Fig. 2B, D). The first precingular plate was large and in contact with plate 1a (Fig. 2D). The first antapical plate (1′′′′) was much smaller than the second antapical plate and displaced to the left (Fig. 2E). The sulcus was composed of an anterior sulcal plate (Sa), a median sulcal plate (Sm), a right sulcal plate (Sd), a left sulcal plate (Ss), and a posterior sulcal plate (Sp) (Fig. 2F). There was a distinct group of pores located on the dorsal side of the second antapical plate, where 10 to 23 pores were arranged in short rows (Fig. 2G). Cells with aberrant plate patterns (e.g., five apical plates, two anterior intercalary plate, five postcingular plates) were observed in the same culture (Fig. S1).

3.2. Molecular analysis and phylogeny

For the LSU sequences, the similarity among the different ribotypes of *A. poporum* ranged from 95.4% to 98.2% and the genetic distances ranged from 0.02 to 0.04. In contrast, the similarity and genetic distances were around 93% and 0.07 at interspecific level (Table 2). For the ITS sequences, the similarity among the different ribotypes of *A. poporum* ranged from 97.1% to 99.2%, and the genetic distances ranged from 0.01 to 0.02. In contrast, at the interspecific level, the similarity and genetic distances were around 91% and 0.08 (Table 3).

The ML and BI analysis that are based on LSU sequences generated similar phylogenetic trees (Fig. 3). Both *Azadinium* and *A. poporum* were monophyletic with maximal support (bootstrap=100% in ML and pp=1.00 in BI, respectively). *Azadinium poporum* comprised 3 well-supported clades, referred to as ribotype A, B,

and C. The strain GM29 was a sister clade of ribotype C with strong support (bootstrap=100% in ML and pp=0.99 in BI, respectively).

The ML and BI analysis based on ITS sequences generated similar phylogenetic trees (Fig. 4). *Azadinium poporum* comprised three well-supported clades, referred to as ribotype A, B, and C. The strain GM29 was a sister clade of ribotype B with maximal support. GM29 belonged to neither ribotype B nor ribotype C and was thus designated as a new ribotype, termed as ribotype D.

3.3. AZA profile

Precursor ion experiments of the typical AZA fragments *m/z* 348, *m/z* 360 and *m/z* 362 were performed to test the presence of AZAs. Whereas the *m/z* 348 and the *m/z* 360 experiments were negative, the *m/z* 362 experiment resulted in two peaks with *m/z* 856 at a retention time of 12.4 min and *m/z* 936 at 11.5 min. The CID spectra of both masses were recorded and resulted in identical spectra to those of AZA-2 and AZA-2 phosphate (Fig. 5). Quantification of both compounds against an external calibration solution of AZA-2 in the Selected Reaction Monitoring (SRM) mode gave an AZA-2 cell quota of 45 ± 1 fg cell^{-1}. AZA-2 phosphate was expressed as AZA-2 equivalent and determined as 0.7 ± 0.5 fg cell^{-1}.

4. Discussion

4.1. Morphology and biogeography

This is the first report of the toxic genus *Azadinium* in waters of the United States. In contrast to the high diversity of *Azadinium* in Europe (up to 9 species) (Tillmann et al., 2009; Tillmann et al., 2014), there are only a few species recovered in Asian waters (*A. poporum*, *A. dalianense*) (Gu et al., 2013; Luo et al., 2013), Argentinean waters (*A.* cf. *spinosum*, *A. poporum* (Akselman and Negri, 2012; Tillmann et al., 2016), the Mexican Pacific (*A. spinosum*) (Hernández-Becerril et al., 2012), and New Zealand waters (*A. poporum*) (Smith et al., 2015), probably because they are small and are not included in most routine monitoring. *A. poporum* seems to be the most widely distributed species with reports from the northeast Atlantic (Tillmann et al., 2010), the northwest Pacific (Potvin et al., 2011; Gu et al., 2013), southwest Atlantic (Argentina, Tillmann et al., 2016) and southwest Pacific (New Zealand, Smith et al., 2015). These species require more attention because of their toxicity, which causes azaspiracid shellfish poisoning (AZP). This occurred through consumption of AZA contaminated mussels that were cultured in Ireland and consumed in several other countries (Satake et al., 1998; Twiner et al., 2008; Klontz et al., 2009). But, as in many countries, the mouse bioassay is still used for seafood control, and azaspiracid shellfish poisoning may have been misidentified as diarrhetic shellfish poisoning (DSP) because the symptoms of both poisonings in mice are the same. Only mass spectral analysis of contaminated shellfish can discriminate between AZP and DSP

297 events. Therefore, insufficient attention has been paid to this group of dinoflagellates
298 in other areas and higher diversities can be expected to be found in the near future.
299 The key morphological characters of the genus *Azadinium* include the
300 presence/absence of an antapical spine, the arrangement of the first precingular plate
301 (whether in contact with the first anterior intercalary plate or not), and the location of
302 the ventral pore (Tillmann et al., 2014). The distinct position of the ventral pore
303 located at the junction of the pore plate and the first two apical plates is characteristic
304 of *A. poporum* (Tillmann et al., 2011), but such a kind of ventral pore was also
305 observed in *A. dalianense* and *A. trinitatum* (Luo et al., 2013; Tillmann et al., 2014). *A.*
306 *dalianense* has only three apical plates and two anterior intercalary plates (Luo et al.,
307 2013), whereas *A. trinitatum* shares an identical plate pattern with that of *A. poporum*
308 (Tillmann et al., 2014). However, *A. trinitatum* has an antapical spine and the left side
309 of the suture po/1′ is farther away from the apical pore than *A. poporum*. Based on the
310 location of the ventral pore and the absence of an antapical spine and configuration of
311 plate 1″, the strain GM29 can be safely classified as *A. poporum*. A group of pores on
312 the dorsal side of the second antapical plate was observed in the Gulf of Mexico strain,
313 which was likewise present in a Korea strain (ribotype B) (Potvin et al., 2011), and
314 many Argentinean and Chinese strains (ribotype C) (Tillmann et al., 2016; Gu
315 personal observations), suggesting that this is a common feature of *A. poporum*
316 although it was not mentioned in the original description. The strain GM29 was
317 obtained by incubating surface sediments from the Gulf of Mexico directly,
318 supporting the idea that *A. poporum* has a cyst stage (Gu et al., 2013), although there

was no direct observation of such a cyst. The cysts might be too small, too inconspicuous and rare, thus escaping microscopic detection during routine plankton surveys and cyst studies so far. In line with previously observations (Gu et al., 2013; Tillmann et al., 2011), the Gulf of Mexico strain *Azadinium poporum* cells also sometimes show aberrant plate patterns in culture.

Before this study, *Azadinium poporum* was reported in the North Sea (ribotype A), Yellow Sea, East China Sea, South China Sea (ribotype B, C), New Zealand (ribotype A) and Argentina (ribotype C) (Tillmann et al., 2011; Gu et al., 2013; Smith et al., 2015; Tillmann et al., 2016). The distribution of *A. poporum* is extended to the Gulf of Mexico, suggesting that this is a widespread species. *A. poporum* of various ribotypes share identical thecate morphology, are relevant to toxicity, and thus highlight the necessity to develop molecular-based assays for targeting all ribotypes.

4.2. Phylogeny and genetic differentiation

The results support the monophyly of the genus *Azadinium* and *A. poporum* (Gu et al., 2013; Tillmann et al., 2014). However, the phylogenetic position of *A. poporum* strain GM29 is not consistent, and forms a sister clade either to ribotype B (LSU) or ribotype C (ITS), whereas phylogenetic positions of other strains of *A. poporum* are consistent. Thus GM29 was recognized as a new ribotype. More ribotypes can be expected as still limited sequences from a few geographical areas are available for this species. Unlike other dinoflagellates, the genetic distances of LSU rDNA among *A. poporum* ribotypes are greater than those of ITS sequences (Tables 2, 3), supporting the idea that LSU is a better fragment for molecular discrimination (Toebe et al.,

2013). However, whether the primers and probes for European *A. poporum* are also applicable for other ribotypes remains to be confirmed.

4.3. Toxin profiles

AZAs have been reported in shellfish of Pacific USA origin, but no details were provided (Trainer et al., 2013). AZA-2 was found in three plankton samples collected in Washington State (northeast Pacific), although neither AZA-1 nor AZA-3 were detected there (Trainer et al., 2013). AZA-1 was the dominant toxin profile in plankton samples collected in the North Sea (Krock et al., 2009), which was later ascribed to *Azadinium spinosum* (Tillmann et al., 2009). For all available *A. spinosum* strains, AZA-2 is present only in conjunction with AZA-1 (Tillmann et al., 2009; Tillmann et al., 2012b). For the potential toxic *A. dexteroporum*, abundance of azaspiracid is very low and neither AZA-1 nor AZA-2 were produced (Percopo et al., 2013). *A. poporum* is the only known *Azadinium* species producing exclusively or predominantly AZA-2 (Krock et al., 2014; Tillmann et al., 2016; present study), thus it is likely responsible for the toxin from the plankton sample collected in Washington State (Trainer et al., 2013). AZAs were also present in shellfish from eastern Canada (Twiner et al., 2008), suggesting that toxic species (e.g., *A. poporum*, A. *spinosum*) might be present there too. In addition, the toxin profile of the *A. poporum* isolate from the Gulf of Mexico is identical with the profile of *A. poporum* from Argentinean shelf waters including the recently discovered AZA-2 phosphate (Tillmann et al., 2016), even though both isolates belong to different ribotypes: C (Argentinean isolate) and D (Gulf of Mexico isolate). In contrast, only AZA-1 was detected in mussels

363 collected from Baja California, Mexico (García-Mendoza et al., 2014), consistent with
364 the fact that *A. spinosum* is present in the Mexican Pacific (Hernández-Becerril et al.,
365 2012). Interestingly, shellfish samples from Morocco (Taleb et al., 2006) and Portugal
366 (Vale et al., 2008) show an AZA-profile with predominant AZA-2, followed by
367 AZA-1, quite different from any shellfish sample from Ireland, Norway, Spain or
368 France (Twiner et al., 2008). Identification of genes involved in saxitoxin biosynthesis
369 contributed to a rapid and accurate molecular method to quantify toxic *Alexandrium*
370 species from marine waters (Murray et al., 2011). However, AZA-related genes have
371 not been identified yet, and their knowledge will contribute to a promising approach
372 for monitoring and studying toxic *Azadinium* in future studies.

373 **5. Conclusions**

374 The first record of *Azadinium poporum* in the Gulf of Mexico supports a wide
375 distribution of this species. Further efforts are needed to examine if it is also present in
376 the Atlantic coast of the USA and Canada. *A. poporum* in the Gulf of Mexico is
377 genetically different from strains from elsewhere, and thus represents a new ribotype.
378 This strain, however, produces predominantly AZA-2 and AZA-2 phosphate, identical
379 to the profiles produced by the Argentinean strains (Tillmann et al., 2016).

380 **Acknowledgements**

381 We thank Urban Tillmann and an anonymous reviewer for constructive suggestions
382 that improved the ms. Haifeng Gu was supported by the National Natural Science
383 Foundation of China (41376170, 41306171) and the Public Science and Technology
384 Research funds projects of Ocean (201305027). Kenneth Neil Mertens is a

385 postdoctoral fellow of FWO Belgium. Andrea M. Price was supported by a Natural
386 Science and Engineering Research Council of Canada (NSERC) doctoral scholarship
387 (CGS-D3). Sample collection was supported by the National Oceanic and
388 Atmospheric Administration, Center for Sponsored Coastal Ocean Research, under
389 award NA09NOS4780204 to Louisiana Universities Marine Consortium and award
390 NA09NOS4780230 to Louisiana State University.
391

391 **References**

392 Adachi, M., Sako, Y., Ishida, Y., 1996. Analysis of *Alexandrium* (Dinophyceae)
393 species using sequences of the 5.8S ribosomal DNA and internal transcribed
394 spacer regions. J. Phycol. 32(3), 424–432.

395 Akselman, R., Negri, R.M., 2012. Blooms of *Azadinium* cf. *spinosum* Elbrächter et
396 Tillmann (Dinophyceae) in northern shelf waters of Argentina, Southwestern
397 Atlantic. Harmful Algae 19, 30–38.

398 Boc, A., Diallo, A.B., Makarenkov, V., 2012. T-REX: A web server for inferring,
399 validating and visualizing phylogenetic trees and networks. Nucleic Acids Res.
400 40(W1), W573–W579.

401 Daugbjerg, N., Hansen, G., Larsen, J., Moestrup, Ø., 2000. Phylogeny of some of the
402 major genera of dinoflagellates based on ultrastructure and partial LSU rDNA
403 sequence data, including the erection of three new genera of unarmoured
404 dinoflagellates. Phycologia 39(4), 302–317.

405 García-Mendoza, E., Sánchez-Bravo, Y.A., Turner, A., Blanco, J., O'Neil, A.,
406 Mancera-Flores, J., Pérez-Brunius, P., Rivas, D., Almazán-Becerril, A.,
407 Peña-Manjarrez, J.L., 2014. Lipophilic toxins in cultivated mussels (*Mytilus*
408 *galloprovincialis*) from Baja California, Mexico. Toxicon 90, 111–123.

409 Gu, H., Luo, Z., Krock, B., Witt, M., Tillmann, U., 2013. Morphology, phylogeny and
410 azaspiracid profile of *Azadinium poporum* (Dinophyceae) from the China Sea.
411 Harmful Algae 21-22, 64–75.

412 Guillard, R.R.L., Ryther, J.H., 1962. Studies of marine planktonic diatoms. I.

Cyclotella nana Hustedt and *Detonula confervacea* Cleve. Can. J. Microbiol. 8(2), 229–239.

Hall, T.A., 1999. BioEdit: a user-friendly biological sequence alignment editor and analysis program for Windows 95/98/NT. Nucleic Acids Symp. Ser. 41, 95–98.

Hernández-Becerril, D.U., Barón-Campis, S.A., Escobar-Morales, S., 2012. A new record of *Azadinium spinosum* (Dinoflagellata) from the tropical Mexican Pacific. Rev. Biol. Mar. Oceanogr. 47(3), 553–557.

Katoh, K., Kuma, K., Toh, H., Miyata, T., 2005. MAFFT version 5: improvement in accuracy of multiple sequence alignment. Nucleic Acids Res. 33(2), 511–518.

Klontz, K.C., Abraham, A., Plakas, S.M., Dickey, R.W., 2009. Mussel-associated azaspiracid intoxication in the United States. Ann. Intern. Med. 150(5), 361.

Krock, B., Tillmann, U., John, U., Cembella, A.D., 2009. Characterization of azaspiracids in plankton size-fractions and isolation of an azaspiracid-producing dinoflagellate from the North Sea. Harmful Algae 8(2), 254–263.

Krock, B., Tillmann, U., Witt, M., Gu, H., 2014. Azaspiracid variability of *Azadinium poporum* (Dinophyceae) from the China Sea. Harmful Algae 36, 22–28.

Lopez-Rivera, A., O'Callaghan, K., Moriarty, M., O'Driscoll, D., Hamilton, B., Lehane, M., James, K., Furey, A., 2010. First evidence of azaspiracids (AZAs): A family of lipophilic polyether marine toxins in scallops (*Argopecten purpuratus*) and mussels (*Mytilus chilensis*) collected in two regions of Chile. Toxicon 55(4), 692–701.

Luo, Z., Gu, H., Krock, B., Tillmann, U., 2013. *Azadinium dalianense*, a new

435 dinoflagellate species from the Yellow Sea, China. Phycologia 52(6), 625–636.
436 Murray, S.A., Wiese, M., Stüken, A., Brett, S., Kellmann, R., Hallegraeff, G., Neilan,
437 B.A., 2011. sxtA-based quantitative molecular assay to identify
438 saxitoxin-producing harmful algal blooms in marine waters. Appl. Environ.
439 Microbiol. 77(19), 7050–7057.
440 Nézan, E., Tillmann, U., Bilien, G., Boulben, S., Chèze, K., Zentz, F., Salas, R.,
441 Chomérat, N., 2012. Taxonomic revision of the dinoflagellate *Amphidoma*
442 *caudata*: transfer to the genus *Azadinium* (Dinophyceae) and proposal of two
443 varieties, based on morphological and molecular phylogenetic analyses. J.
444 Phycol. 48(4), 925–939.
445 Percopo, I., Siano, R., Rossi, R., Soprano, V., Sarno, D., Zingone, A., 2013. A new
446 potentially toxic *Azadinium* species (Dinophyceae) from the Mediterranean Sea,
447 *A. dexteroporum* sp. nov. J. Phycol. 49(5), 950–966.
448 Posada, D., 2008. jModelTest: Phylogenetic model averaging. Mol. Biol. Evol. 25(7),
449 1253–1256.
450 Potvin, É., Jeong, H.J., Kang, N.S., Tillmann, U., Krock, B., 2011. First report of the
451 photosynthetic dinoflagellate genus *Azadinium* in the Pacific Ocean:
452 Morphology and molecular characterization of *Azadinium* cf. *poporum*. J.
453 Eukaryot. Microbiol. 59(2), 145–156.
454 Ronquist, F., Huelsenbeck, J.P., 2003. MrBayes 3: Bayesian phylogenetic inference
455 under mixed models. Bioinformatics 19(12), 1572–1574.
456 Satake, M., Ofuji, K., Naoki, H., James, K.J., Furey, A., McMahon, T., Silke, J.,

457 Yasumoto, T., 1998. Azaspiracid, a new marine toxin having unique spiro ring
458 assemblies, isolated from Irish mussels, *Mytilus edulis*. J. Am. Chem. Soc.
459 120(38), 9967–9968.
460 Scholin, C.A., Herzog, M., Sogin, M., Anderson, D.M., 1994. Identification of group-
461 and strain-specific genetic markers for globally distributed *Alexandrium*
462 (Dinophyceae). II. Sequence analysis of a fragment of the LSU rRNA gene. J.
463 Phycol. 30(6), 999–1011.
464 Smith K.F., Rhodes L., Harwood D.T., Adamson J., Moisan C., Munday R., Tillmann U.,
465 2015. Detection of *Azadinium poporum* in New Zealand: the use of molecular
466 tools to assist with species isolations. J. Appl. Phycol. In press.
467 Stamatakis, A., 2006. RAxML-VI-HPC: maximum likelihood-based phylogenetic
468 analyses with thousands of taxa and mixed models. Bioinformatics 22(21),
469 2688–2690.
470 Taleb, H., Vale, P., Amanhir, R., Benhadouch, A., Sagou, R., Chafik, A., 2006. First
471 detection of azaspiracids in mussels in north west Africa. J. Shellfish Res. 25(3),
472 1067–1070.
473 Tillmann, U., Elbrächter, M., Krock, B., John, U., Cembella, A., 2009. *Azadinium*
474 *spinosum* gen. et sp. nov. (Dinophyceae) identified as a primary producer of
475 azaspiracid toxins. Eur. J. Phycol. 44(1), 63–79.
476 Tillmann, U., Elbrächter, M., John, U., Krock, B., Cembella, A., 2010. *Azadinium*
477 *obesum* (Dinophyceae), a new nontoxic species in the genus that can produce
478 azaspiracid toxins. Phycologia 49(2), 169–182.

Tillmann, U., Elbrächter, M., John, U., Krock, B., 2011. A new non-toxic species in the dinoflagellate genus *Azadinium*: ***A. poporum*** sp. nov. Eur. J. Phycol. 46(1), 74–87.

Tillmann, U., Salas, R., Gottschling, M., Krock, B., O'Driscoll, D., Elbrächter, M., 2012a. *Amphidoma languida* sp. nov. (Dinophyceae) reveals a close relationship between *Amphidoma* and *Azadinium*. Protist 163(5), 701–719.

Tillmann, U., Soehner, S., Nézan, E., Krock, B., 2012b. First record of the genus *Azadinium* (Dinophyceae) from the Shetland Islands, including the description of *Azadinium polongum* sp. nov. Harmful Algae 20, 142–155.

Tillmann, U., Gottschling, M., Nézan, E., Krock, B., Bilien, G., 2014. Morphological and molecular characterization of three new *Azadinium* species (Amphidomataceae, Dinophyceae) from the Irminger Sea. Protist 165(4), 417–444.

Tillmann, U., Borel, C. M., Barrera, F., Lara, R., Krock, B., Almandoz, G. O., Witt, M., Trefault, N., 2016. *Azadinium poporum* from the Argentine continental shelf, southwestern Atlantic, produces azaspiracid-2 and azaspiracid-2 phosphate. Harmful Algae 51: 40–55.

Toebe, K., Joshi, A.R., Messtorff, P., Tillmann, U., Cembella, A., John, U., 2013. Molecular discrimination of taxa within the dinoflagellate genus *Azadinium*, the source of azaspiracid toxins. J. Plankton Res. 35(1), 225–230.

Trainer, V.L., Moore, L., Bill, B.D., Adams, N.G., Harrington, N., Borchert, J., Da Silva, D.A., Eberhart, B.T.L., 2013. Diarrhetic shellfish toxins and other

lipophilic toxins of human health concern in Washington State. Mar. Drugs 11(6), 1815–1835.

Twiner, M.J., Rehmann, N., Hess, P., Doucette, G.J., 2008. Azaspiracid shellfish poisoning: a review on the chemistry, ecology, and toxicology with an emphasis on human health impacts. Mar. Drugs 6(2), 39–72.

Ueoka, R., Ito, A., Izumikawa, M., Maeda, S., Takagi, M., Shin-ya, K., Yoshida, M., van Soest, R.W.M., Matsunaga, S., 2009. Isolation of azaspiracid-2 from a marine sponge *Echinoclathria* sp. as a potent cytotoxin. Toxicon 53(6), 680–684.

Vale, P., Bire, R., Hess, P., 2008. Confirmation by LC-MS/MS of azaspiracids in shellfish from the Portuguese north-western coast. Toxicon 51(8), 1449–1456.

Yao, J., Tan, Z., Zhou, D., Guo, M., Xing, L., Yang, S., 2010. Determination of azaspiracid-1 in shellfishes by liquid chromatography with tandem mass spectrometry. Chin. J. Chromatogr. 28(4), 363–367 (in Chinese).

Figure captions

Fig. 1. LM of live cells of *Azadinium poporum* strain GM29. (A) Ventral view, showing a large nucleus (N) and several pyrenoids (P). (B) Ventral view, showing a putative large chloroplast. (C) Ventral view, showing a large nucleus (Sybr Green staining).

Fig. 2. A scanning electron micrograph of vegetative cells of *Azadinium poporum* strain GM29. (A) Ventral view, showing the conical epitheca and round hypotheca. (B) Dorsal view, showing three anterior intercalary plates (1a, 2a, 3a). (C) Apical view, showing the first apical plate (1′), pore plate (po), cover plate (cp) and ventral pore (vp). (D) Apical view, showing four apical plates (1′-4′), three intercalary plates and six precingular plates (1″-6″). (E) Antapical view, showing six postcingular plates (1‴-6‴) and two antapical plates (1⁗, 2⁗) of unequal size. (F) Detail of plate 2⁗, showing a group of pores on the dorsal side. (G) Sulcal plates, showing an anterior sulcal plate (Sa), a median sulcal plate (Sm), a right sulcal plate (Sd), a left sulcal plate (Ss), and a posterior sulcal plate (Sp).

Fig. 3. Phylogeny of *Azadinium poporum* inferred from partial LSU rDNA sequences using maximum likelihood (ML). Branch lengths are drawn to scale, with the scale bar indicating the number of nucleotide substitutions per site. Numbers on branches are statistical support values to clusters on the right of them (left: ML

bootstrap support values; right: Bayesian posterior probabilities).

Fig. 4. Phylogeny of *Azadinium poporum* inferred from ITS and 5.8S rDNA sequences using maximum likelihood (ML). Branch lengths are drawn to scale, with the scale bar indicating the number of nucleotide substitutions per site. Numbers on branches are statistical support values to clusters on the right of them (left: ML bootstrap support values; right: Bayesian posterior probabilities).

Fig. 5. (A) Selected Ion traces of *Azadinium poporum* strain GM029: m/z 856>672 for AZA-2 and m/z936>918 for AZA-2 phosphate. (B) Collision induced dissociation (CID) spectrum of m/z 856 (AZA-2). (C) CID spectrum of m/z936 (AZA-2 phosphate).

Fig. S1. A scanning electron micrograph of abnormal vegetative cells of *Azadinium poporum* strain GM29. (A) Apical view, showing five apical plates. (B) Apical view, showing two anterior intercalary plates. (C) Antapical view, showing five postcingular plates.

Table 1. Mass transitions m/z (Q1>Q3 mass) and their respective AZAs.

Mass transition	Toxin	Collision energy (CE) [V]
716>698	AZA-33	40
816>798	AZA-39	40
816>348	AZA-39	70
828>658	AZA-3	70
828>810	AZA-3	40
830>812	AZA-38	40
830>348	AZA-38	70
842>672	AZA-1	70
842>824	AZA-1, AZA-41	40
844>826	AZA-4, AZA-5	40
846>828	AZA-37	40
856>672	AZA-2	70
856>838	AZA-2	40
858>840	AZA-7, AZA-8, AZA-9, AZA-10, AZA-36	40
868>362	Undescribed	70
870>852	Me-AZA-2	40
872>854	AZA-11, AZA-12	40
936>918	AZA-2 phosphate	40

Table 2. Partial LSU sequences comparison of *Azadinium poporum* strain GM29 from the Gulf of Mexico with those of related species from elsewhere. The percentage refers to the similarity out of partial LSU sequences (701bp); the numeral in brackets refers to pairwise genetic distance.

	GM29	G25	G66	G42	UTHC5	AZCH02
GM29 (ribotype D)	-					
G25 (ribotype B)	97.7%(0.02)	-				
G66 (ribotype B)	97.8%(0.02)	98.2%(0.02)	-			
G42 (ribotype C)	98.2%(0.02)	97.7%(0.02)	97.5%(0.02)	-		
UTHC5 (ribotype A)	95.4%(0.04)	96.2%(0.04)	96.4%(0.03)	96.5%(0.03)	-	
AZCH02 (*A. dalianense*)	92.7%(0.07)	91.7%(0.08)	92.2%(0.07)	93.2%(0.06)	92.7%(0.06)	-

Table 3. ITS sequences comparison of *Azadinium poporum* strain GM29 from the Gulf of Mexico with those of related species from elsewhere.

The percentage refers to the similarity out of ITS region sequences; the numeral in bracket refers to pairwise genetic distance.

	GM29	G25	G66	G42	UTHC5	AZCH02
GM29 (ribotype D)	-					
G25 (ribotype B)	98.8%(0.01)	-				
G66 (ribotype B)	98.7%(0.01)	99.2%(0.01)	-			
G42 (ribotype C)	98.4%(0.02)	98.2%(0.02)	97.7%(0.02)	-		
UTHC5 (ribotype A)	97.6%(0.02)	97.3%(0.02)	97.1%(0.02)	97.3%(0.02)	-	
AZCH02 (*A. dalianense*)	90.8%(0.08)	90.6%(0.08)	90.8%(0.08)	90.6%(0.08)	91.3%(0.08)	-

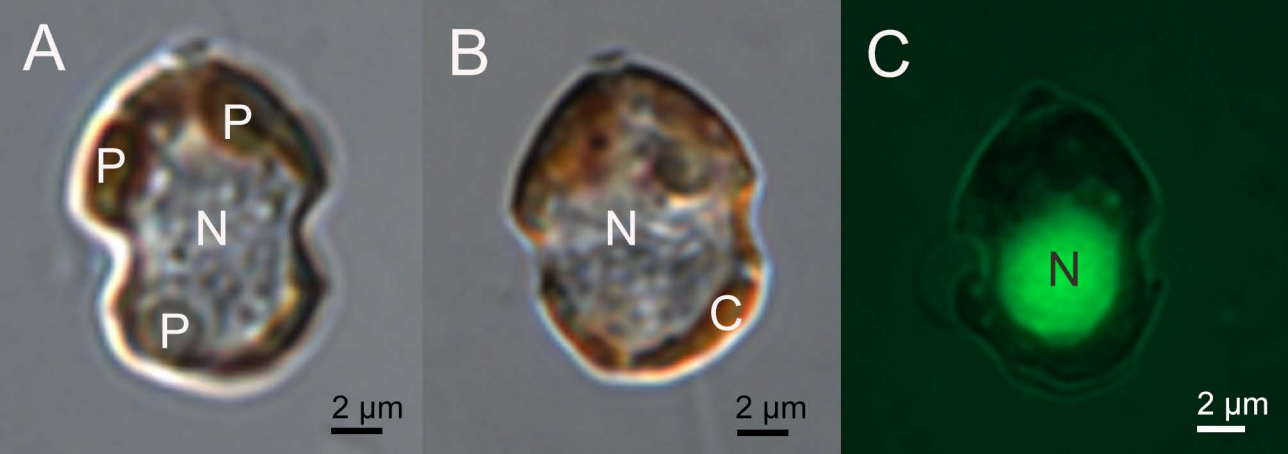
A
P
P
N
P
2 µm
B
N
C
2 µm
C
N
2 µm

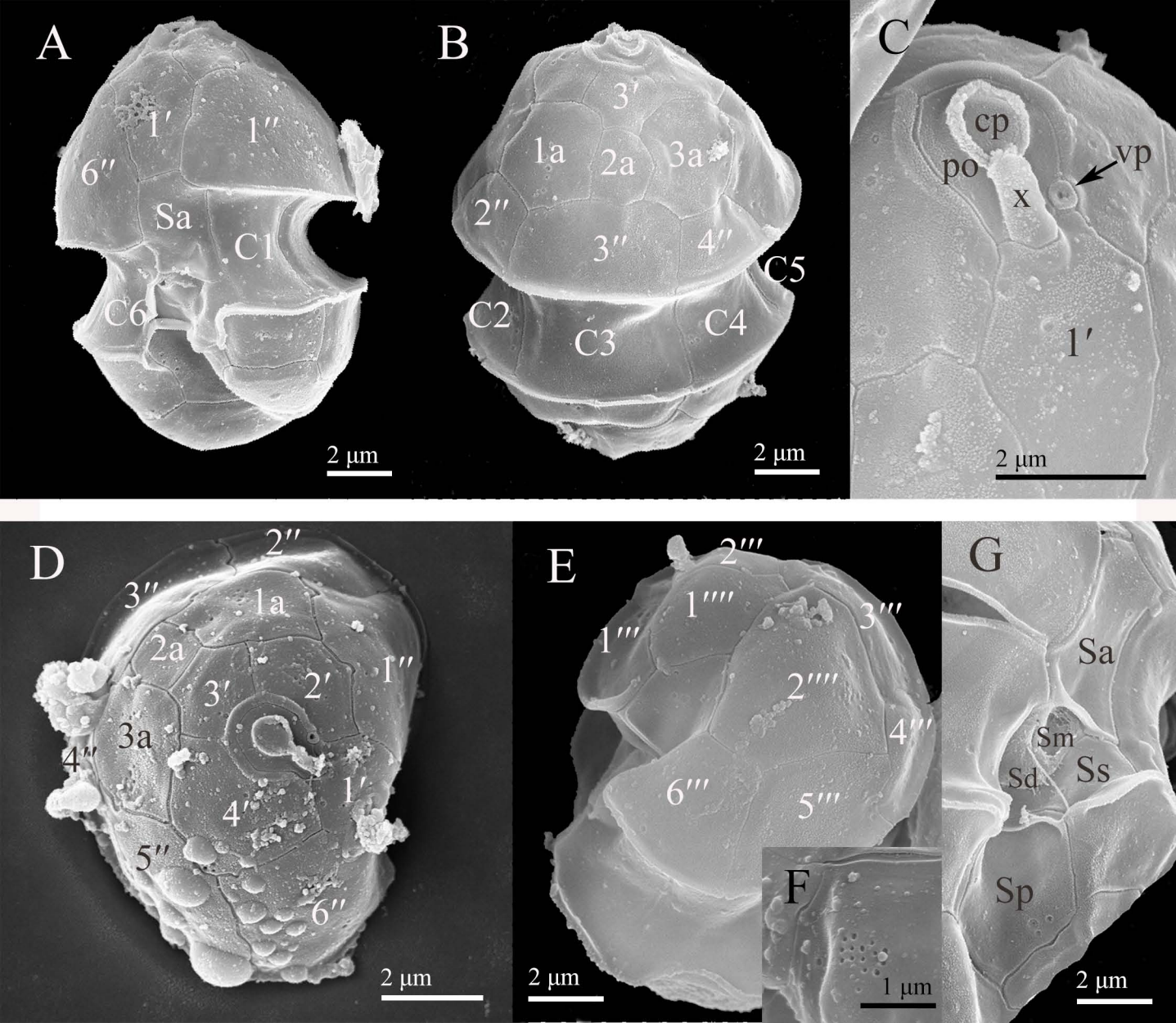
A
1′
1″
6″
Sa
C1
C6
2 µm
B
3′
1a
2a
3a
2″
3″
4″
C5
C2
C3
C4
2 µm
C
cp
po
vp
x
1′
2 µm
D
2″
3″
1a
2a
1″
3′
2′
3a
4″
1′
4′
5″
6″
2 µm
E
2‴
1⁗
1‴
3‴
2⁗
4‴
6‴
5‴
2 µm
F
1 µm
G
Sa
Sm
Sd
Ss
Sp
2 µm

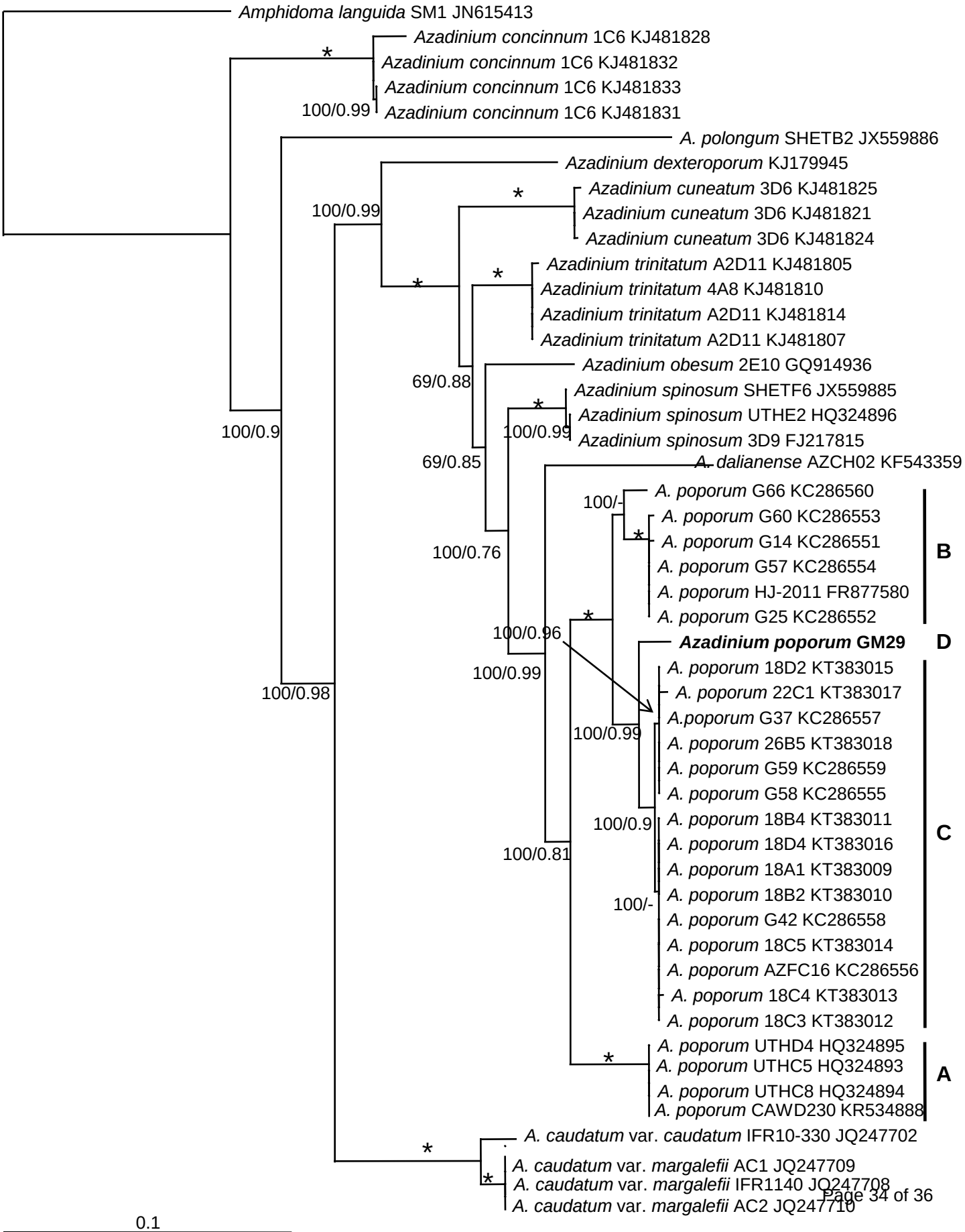
Amphidoma languida SM1 JN615413
Azadinium concinnum 1C6 KJ481828
Azadinium concinnum 1C6 KJ481832
Azadinium concinnum 1C6 KJ481833
Azadinium concinnum 1C6 KJ481831
A. polongum SHETB2 JX559886
Azadinium dexteroporum KJ179945
Azadinium cuneatum 3D6 KJ481825
Azadinium cuneatum 3D6 KJ481821
Azadinium cuneatum 3D6 KJ481824
Azadinium trinitatum A2D11 KJ481805
Azadinium trinitatum 4A8 KJ481810
Azadinium trinitatum A2D11 KJ481814
Azadinium trinitatum A2D11 KJ481807
Azadinium obesum 2E10 GQ914936
Azadinium spinosum SHETF6 JX559885
Azadinium spinosum UTHE2 HQ324896
Azadinium spinosum 3D9 FJ217815
A. dalianense AZCH02 KF543359
A. poporum G66 KC286560
A. poporum G60 KC286553
A. poporum G14 KC286551
A. poporum G57 KC286554
A. poporum HJ-2011 FR877580
A. poporum G25 KC286552
Azadinium poporum GM29
A. poporum 18D2 KT383015
A. poporum 22C1 KT383017
A.poporum G37 KC286557
A. poporum 26B5 KT383018
A. poporum G59 KC286559
A. poporum G58 KC286555
A. poporum 18B4 KT383011
A. poporum 18D4 KT383016
A. poporum 18A1 KT383009
A. poporum 18B2 KT383010
A. poporum G42 KC286558
A. poporum 18C5 KT383014
A. poporum AZFC16 KC286556
A. poporum 18C4 KT383013
A. poporum 18C3 KT383012
A. poporum UTHD4 HQ324895
A. poporum UTHC5 HQ324893
A. poporum UTHC8 HQ324894
A. poporum CAWD230 KR534888
A. caudatum var. caudatum IFR10-330 JQ247702
A. caudatum var. margalefii AC1 JQ247709
A. caudatum var. margalefii IFR1140 JQ247708
A. caudatum var. margalefii AC2 JQ247710
100/0.99
100/0.99
100/0.9
69/0.88
100/0.99
69/0.85
100/-
100/0.76
100/0.96
100/0.99
100/0.98
100/0.99
100/0.9
100/0.81
100/-
B
D
C
A
0.1

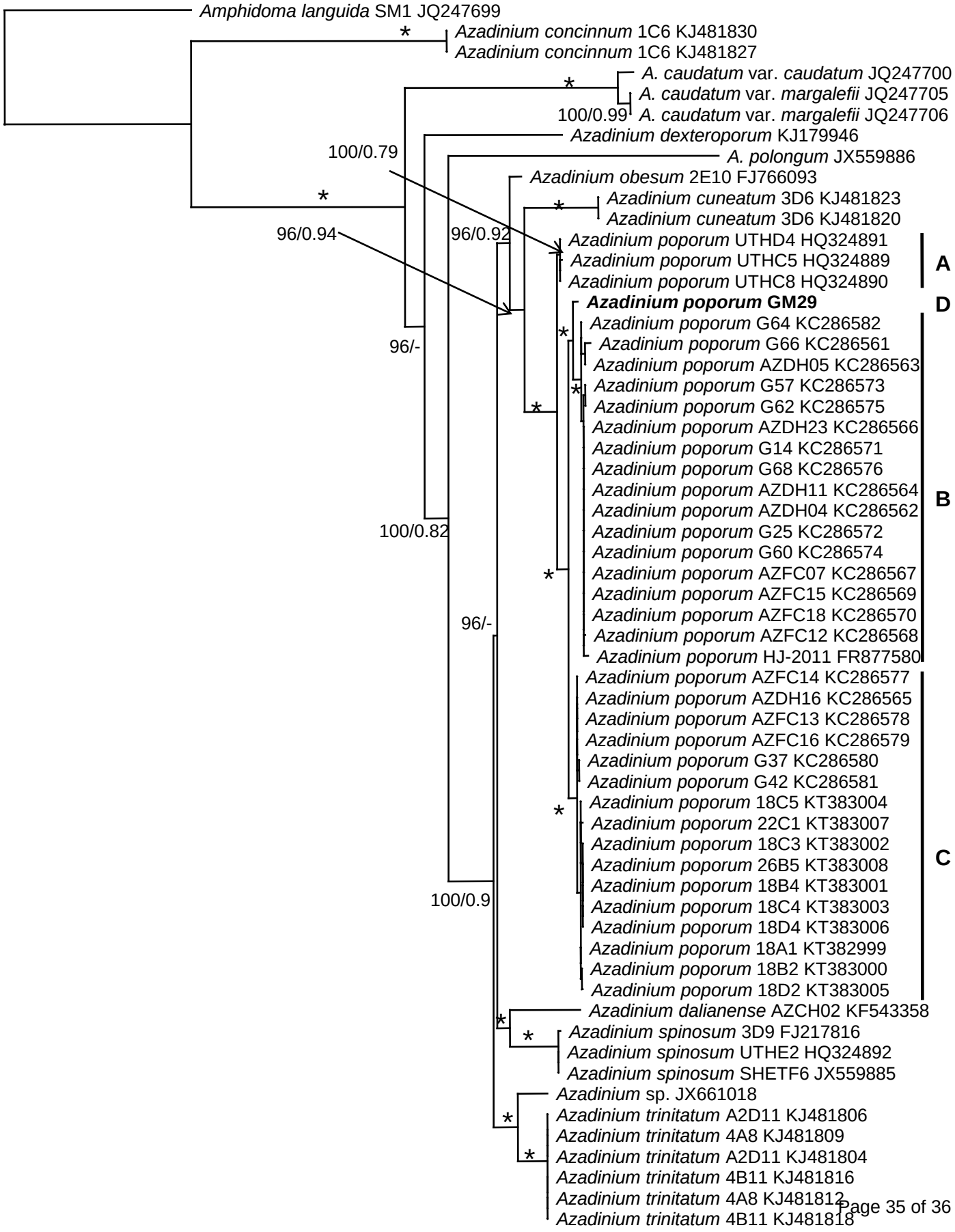
Amphidoma languida SM1 JQ247699
Azadinium concinnum 1C6 KJ481830
Azadinium concinnum 1C6 KJ481827
A. caudatum var. *caudatum* JQ247700
A. caudatum var. *margalefii* JQ247705
100/0.99
A. caudatum var. *margalefii* JQ247706
Azadinium dexteroporum KJ179946
100/0.79
A. polongum JX559886
Azadinium obesum 2E10 FJ766093
Azadinium cuneatum 3D6 KJ481823
Azadinium cuneatum 3D6 KJ481820
96/0.94
96/0.92
Azadinium poporum UTHD4 HQ324891
Azadinium poporum UTHC5 HQ324889
Azadinium poporum UTHC8 HQ324890
A
***Azadinium poporum* GM29**
D
Azadinium poporum G64 KC286582
96/-
Azadinium poporum G66 KC286561
Azadinium poporum AZDH05 KC286563
Azadinium poporum G57 KC286573
Azadinium poporum G62 KC286575
Azadinium poporum AZDH23 KC286566
Azadinium poporum G14 KC286571
Azadinium poporum G68 KC286576
Azadinium poporum AZDH11 KC286564
Azadinium poporum AZDH04 KC286562
B
100/0.82
Azadinium poporum G25 KC286572
Azadinium poporum G60 KC286574
Azadinium poporum AZFC07 KC286567
Azadinium poporum AZFC15 KC286569
96/-
Azadinium poporum AZFC18 KC286570
Azadinium poporum AZFC12 KC286568
Azadinium poporum HJ-2011 FR877580
Azadinium poporum AZFC14 KC286577
Azadinium poporum AZDH16 KC286565
Azadinium poporum AZFC13 KC286578
Azadinium poporum AZFC16 KC286579
Azadinium poporum G37 KC286580
Azadinium poporum G42 KC286581
Azadinium poporum 18C5 KT383004
Azadinium poporum 22C1 KT383007
Azadinium poporum 18C3 KT383002
Azadinium poporum 26B5 KT383008
C
100/0.9
Azadinium poporum 18B4 KT383001
Azadinium poporum 18C4 KT383003
Azadinium poporum 18D4 KT383006
Azadinium poporum 18A1 KT382999
Azadinium poporum 18B2 KT383000
Azadinium poporum 18D2 KT383005
Azadinium dalianense AZCH02 KF543358
Azadinium spinosum 3D9 FJ217816
Azadinium spinosum UTHE2 HQ324892
Azadinium spinosum SHETF6 JX559885
Azadinium sp. JX661018
Azadinium trinitatum A2D11 KJ481806
Azadinium trinitatum 4A8 KJ481809
Azadinium trinitatum A2D11 KJ481804
Azadinium trinitatum 4B11 KJ481816
Azadinium trinitatum 4A8 KJ481812
Azadinium trinitatum 4B11 KJ481818
0.1